Science of the Total Environment 653 (2019) 431–445

Contents lists available at ScienceDirect

Science of the Total Environment

journal homepage: www.elsevier.com/locate/scitotenv

Modeling the effect of land use and climate change on water resources and soil erosion in a tropical West African catch-ment (Dano, Burkina Faso) using SHETRAN

Felix Op de Hipt [a,*], Bernd Diekkrüger [a], Gero Steup [a], Yacouba Yira [a], Thomas Hoffmann [b], Michael Rode [c], Kristian Näschen [a]

[a] Department of Geography, University of Bonn, Meckenheimer Allee 166, 53115 Bonn, Germany
[b] German Federal Institute of Hydrology, Am Mainzer Tor 1, 56068 Koblenz, Germany
[c] Helmholtz Center for Environmental Research – UFZ, Brückstraße 3a, 39114 Magdeburg, Germany

HIGHLIGHTS

- Past and future LULC maps suggest an increase of cropland at the expense of savanna.
- The changing LULC leads to increasing surface runoff and suspended sediment yield.
- Climate change leads to increasing surface runoff and suspended sediment yield.
- Combined changes of climate and LULC leads to increased runoff and sediment yield

GRAPHICAL ABSTRACT

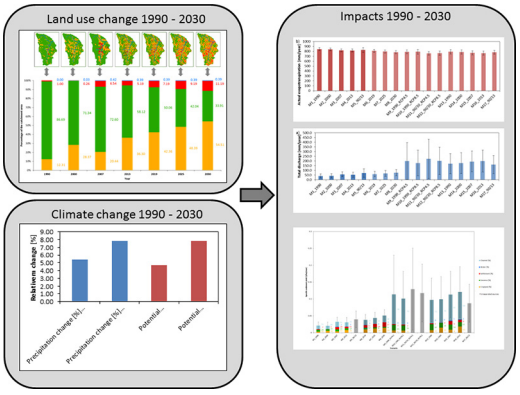

ARTICLE INFO

Article history:
Received 12 January 2018
Received in revised form 22 October 2018
Accepted 26 October 2018
Available online 28 October 2018

Editor: Ralf Ludwig

Keywords:
Hydrological modeling
Erosion modeling
Climate change
Land use change

ABSTRACT

This study investigates the effect of land use and land cover (LULC) and climate change on catchment hydrology and soil erosion in the Dano catchment in south-western Burkina Faso based on hydrological and soil erosion modeling. The past LULC change is studied using land use maps of the years 1990, 2000, 2007 and 2013. Based on these maps future LULC scenarios were developed for the years 2019, 2025 and 2030. The observed past and modeled future LULC are used to feed SHETRAN, a hydrological and soil erosion model. Observed and modeled climate data cover the period 1990–2030.

The isolated influence of LULC change assuming a constant climate is simulated by applying the seven LULC maps under observed climate data of the period 1990–2015. The isolated effect of climate scenarios (RCP4.5 and 8.5 of CCLM4–8) is studied by applying the LULC map of 1990 to the period 1990–2032. Additionally, we combined past modeled climate data and past observed LULC maps. Two chronological and continuous simulations were used to estimate the impact of LULC in the past and in the future by gradually applying the LULC maps. These simulations consider the combined impact of LULC and climate change.

The simulations that assumed a constant climate and a changing LULC show increasing water yield (3.6%–46.5%) and mainly increasing specific sediment yield (−3.3%–52.6%). The simulations that assume constant LULC and climate as changing factor indicate increases in water yield of 24.5% to 46.7% and in sediment yield of 31.1% to

* Corresponding author.
E-mail address: opdehipt@bafg.de (F. Op de Hipt).

https://doi.org/10.1016/j.scitotenv.2018.10.351
0048-9697/

54.7% between the periods 1990–2005 and 2006–2032. The continuous simulations signal a clear increase in water yield (20.3%–73.4%) and specific sediment yield (24.7% to 90.1%). Actual evapotranspiration is estimated to change by between −7.3% (only LUCC) to +3.3% (only climate change). When comparing observed LULC and climate change alone, climate change has a larger impact on discharge and sediment yield, but LULC amplifies climate change impacts strongly. However, future LULC (2019–2030) will have a stronger impact as currently observed.

1. Introduction

Population and economic growth are considered to be the most important drivers of land degradation. Human-driven land use and land cover (LULC) changes influence water resources and may intensify land degradation by water-related soil erosion and nutrient depletion (CILSS, 2016; UNEP, 2012). Especially in countries with fragile ecosystems, limited water and soil resources, changes in the hydrological cycle through LULC and climate changes may lead to an increased flood and drought risk as well as accelerated soil erosion rates. Understanding the effect of LULC and climate change on water and soil resources is paramount especially in countries, such as Burkina Faso, whose societies are highly dependent on rain-fed agriculture.

The population in Burkina Faso is growing at annual rates of about 3% in the last decade (The World Bank, 2017). The growing food demand and the expansion of settlement areas lead to LULC change through the conversion of savanna vegetation to cropland and settlement area. The increased pressure on soil resources reduces the agricultural production through nutrient depletion and loss of fertile soil through soil erosion (CILSS, 2016). Assessing the long term impact of LULC change on runoff generation and soil erosion is therefore important for decision makers to plan environmental protection measures. However, the number of studies that investigate feedback mechanisms between LULC change, runoff generation and soil erosion is limited in West Africa.

Hydrological processes and soil erosion are closely linked and strongly controlled by LULC. Sustainable management of water and soil resources require a combined consideration of water and sediment fluxes (Diekkrüger, 2010). LULC change impacts can be studied by comparing field measurements of hydrological and soil erosion variables from different LULC classes (Braimoh and Vlek, 2004; Giertz et al., 2010, 2005; Hiepe, 2008). Field measurements show that a change from savanna or forest vegetation to cropland can reduce soil hydraulic conductivity and increased surface runoff and soil erosion. This can be explained by the reduction of macroporosity as result of decreased biological activity following the disturbance of the soil by agricultural activities (Giertz et al., 2005). However, measurement of soil erosion is often not possible over the required temporal and spatial scale. Field studies have therefore to be complemented by hydrological and soil erosion modeling studies. Hydrological and soil erosion models have been used to predict the effect of land use and climate change on soil erosion and to identify hot spots of soil erosion that require erosion control measures (Bossa et al., 2014; Hiepe, 2008; Pandey et al., 2016). If available, LULC maps from different years may be used as input into hydrological and soil erosion models to simulate the effect on runoff and soil erosion. Increased runoff and soil erosion rates are often predicted by hydrological and soil erosion models if the natural vegetation is converted to arable land (Bossa, 2012; Hiepe, 2008; Yira et al., 2016).

Different model concepts exist (empirical, conceptual and physically based models) among which physically based spatially distributed models are considered suitable for the analyses of LULC impacts on erosion at smaller scales as a certain complexity is necessary for the predictions of the changing LULC conditions (Pandey et al., 2016). The parameter values of these model types have a physical meaning and therefore can be better estimated, which increases the quality of the simulated output (de Vente et al., 2013; Merritt et al., 2003; Pandey et al., 2016). The hydrological and soil erosion model SHETRAN (Birkinshaw et al., 2010b; Ewen et al., 2000) has been successfully applied to simulate effects of changing LULC (Bathurst et al., 2011; Lukey et al., 2000, 1995) and climate (Op de Hipt et al., 2018). SHETRAN studies used several approaches to investigate the impacts of a changing LULC. On the one hand, hypothetical scenarios derived from a simple change of vegetation properties (Bathurst et al., 2011, 2005; Birkinshaw et al., 2010a; Lukey et al., 2000, 1995) are used and on the other hand the analyses of observed land use in different catchments were compared to reflect changed LULC (Elliott et al., 2011). One novelty of the present study is therefore the combined investigation of observed and future LULC change in the same catchment over >20 years using SHETRAN.

The LULC change in the catchment is driven by a high population growth rate (3% per year) leading to the expansion of cropland at the expense of savanna as it is frequently observed in West Africa (CILSS, 2016; Codjoe, 2004; Yira et al., 2016). The principle motivation of the present study is to fill the knowledge gap regarding the impact of LULC change on runoff generation and soil erosion. Studies on these topics are rather limited in West Africa but work on the impact of LULC change on hydrological processes (Yira et al., 2016) and on the general modeling of soil erosion without changing LULC influences (Op de Hipt et al., 2017; Schmengler, 2010) in the present study catchment exist. Despite these studies a clear knowledge gap was identified regarding the assessment of past and future impacts of LULC change on soil erosion. Furthermore, the combined consideration of LULC and climate change is frequently identified as future research objective (Op de Hipt et al., 2018; Yira, 2016). We aim to fill this gap by a combined assessment of LULC and climate change over a period of 40 years (1990–2030). The SHETRAN model was set up to simulate and to evaluate the impacts of these changes. SHETRAN was already calibrated and validated in the present study catchment (Op de Hipt et al., 2017).

The major aims of this study are, to:

1. Investigate the observed past and the modeled future LULC change using seven land use maps.
2. Assess the isolated and combined impact of LULC and climate change on simulated mean annual water yield and mean annual actual evapotranspiration.
3. Examine the isolated and combined effect of LULC and climate change on mean annual suspended sediment yield and compare the contribution of different sediment sources (land use, channel, hillslope).

2. Methods

2.1. Study area

The studied catchment has a size of 126 km^2 and is located in the south-west of Burkina Faso, West Africa (Fig. 1). The study site is part of three focal watersheds of the WASCAL program (West African Science Service Center on Climate Change and Adapted Land Use, www.wascal.org). WASCAL is a multidisciplinary program investigating the influence of climate and land use/land cover change on human and environmental systems.

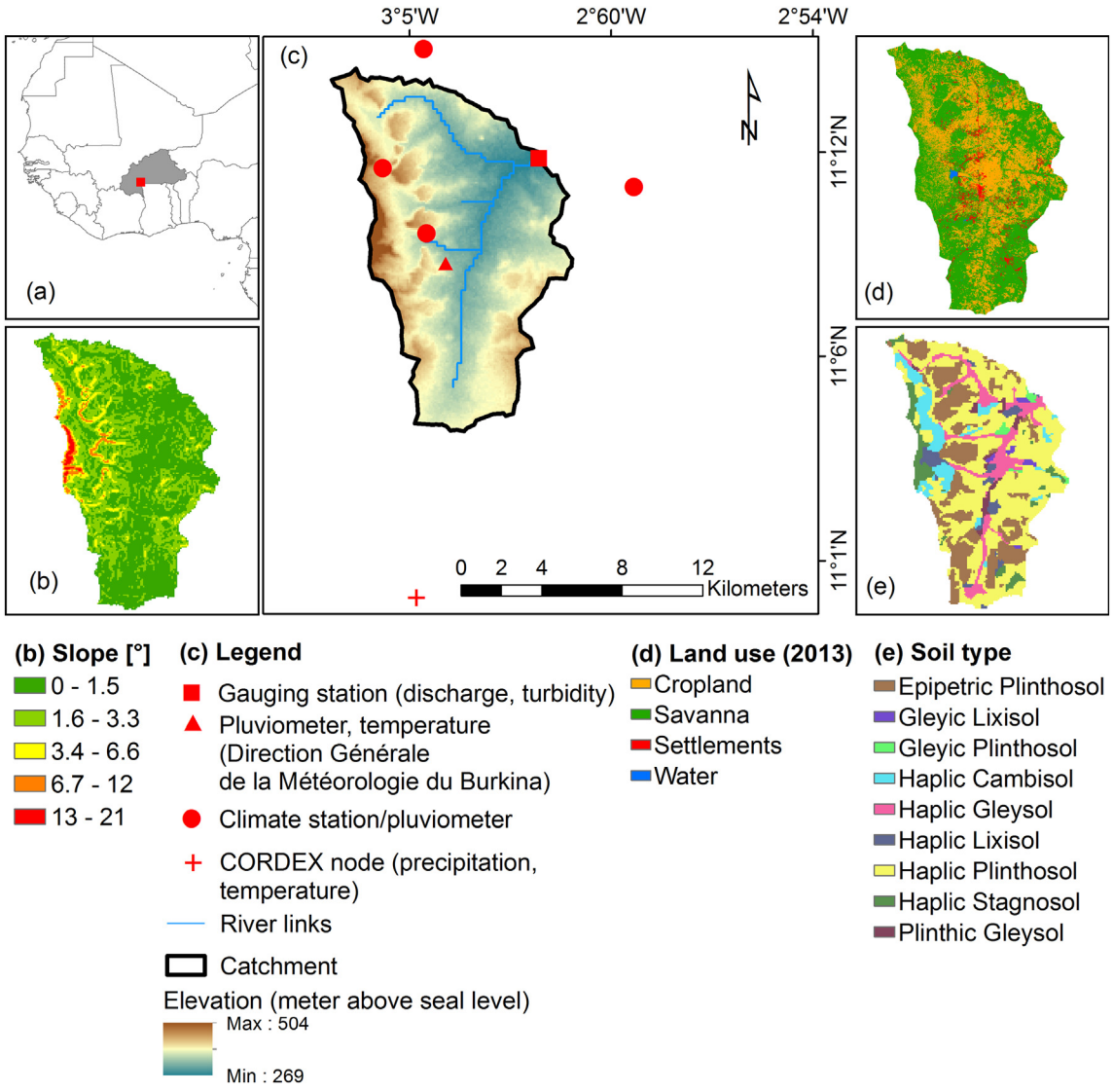

Fig. 1. Location map of the Dano catchment: (a) location of the catchment and Burkina Faso in West Africa, (b) slope of the catchment, (c) model catchment, (d) land use map (Forkuor, 2014), (e) soil map (data base: soil survey done by Ozias Hounkpatin, Soil Science of Institute of Crop Science and Resource Conservation, University Bonn). DGM refers to the Direction Générale de la Météorologie du Burkina.

The watershed is characterized by a slightly undulating landscape with low slope gradients (average and maximum gradients are 1.8° and 21°, respectively, Fig. 1b) and an elevation (Fig. 1c) ranging from 269 to 504 m above sea level (masl). Annual precipitation range from 800 to 1200 mm/a for the period 1951–2005 (Schmengler, 2010). The annual rainfall dynamic is characterized by a distinct rainy season (May to October) and a dry season from November to April.

Soils are dominated by plinthosols (73%) according to the World Reference Base (WRB) for soil resources (IUSS Working Group, 2006). Plinthosols are characterized by high content of coarse particles and a plinthic subsurface layer. Soils of the valley bottoms are mainly gleysols. Other soils formed in the region are cambisols, lixisols, leptosols and stagnosols (Fig. 1e).

The natural vegetation is characterized by the Sudanian region with wood, shrub and arboraceous savanna and abundant annual grasses. The growing population and the resulting demand for cropland and settlements lead to a reduction of the savanna vegetation (Yira et al., 2016). The dominant cultivated crops are sorghum (*Sorghum bicolor*), millet (*Pennisetum glaucum*), maize (*Zea mays*), cowpeas (*Vigna unguiculata*) and groundnut (*Arachidis hypogaea*). Cotton (*Gossypium hirsutum*) is the main cash crop.

2.2. Data sources and processing

The modeling of changing surface runoff and soil erosion requires past, present and future climate and land use data as model inputs.

2.2.1. Land use data

2.2.1.1. Observed LULC maps. Observed LULC maps from four different years (LULC_1990, LULC_2000, LULC_2007, LULC_2013) were available to assess the past impact of LULC change on hydrology and soil erosion. The three maps that show the status from 1990 to 2007 were derived from Landsat TM (http://glovis.usgs.gov/) and MODIS (https://mrtweb.cr.usgs.gov/) images by Landmann et al. (2007). The map of 2013 compiled by Forkuor (2014) is based on Landsat TM and RapidEye images (https://www.planet.com/products/#satellite-imagery). As the maps are available at different resolutions, they were resampled using the majority filter to match the resolution of 200 m. Both studies used the Land Cover Classification System (LCCS) from the Food and Agricultural Organization (FAO).

In order to homogenize the LULC classes for each of the four maps, the LULC classes of the years 1990 to 2007 were reclassified to match

the LULC map of the year 2013. The reclassification was done based on the approach described in Yira et al. (2016): Classes with similar characteristics regarding seasonality of vegetation cover and hydrological properties were grouped (Table 1). The resulting land use maps were used to simulate the effect LULC change on water and soil resources in the past.

2.2.1.2. Future LULC scenarios. Based on the observed LULC changes between 2000 and 2013, future LULC scenarios were developed for the years 2019, 2025 and 2030 (LULC_2019, LULC_2025, LULC_2030) by using the Land Change Modeler (Clark Labs, Clark University, Worcester, USA). The approach used by the Land Change Modeler is based on transition potentials which are calculated using a Multi-Layer Perceptron (MLP) neural network (Chan et al., 2001). The transition potentials for the future depend on the transitions that have already occurred in the past. As explanatory variables several distance maps were used (distance to roads, fields and settlements) as well as spatially autocorrelated maps of the digital elevation model (DEM) and observed disturbances (transitions from savanna to crop or settlements). Finally a stochastic Markov chain technique (Wilson and Weng, 2011) is applied to simulate the probability of LULCC and generate the future land use maps.

As the prediction of the development of areas covered by surface water is difficult based on a very small proportion of grid cells, it was assumed that these areas have not changed since 2013. An overview of the land use classes is given in Table 1.

2.2.2. Climate and hydrological data

Two climate datasets were used in this study.

2.2.2.1. Observed climate and hydrological data. SHETRAN requires various input data to simulate hydrological and soil erosion processes (Table 2). Some of the required data sets are already available from previous studies and from literature. However, in order to calibrate and validate the model (see Section 2.3.1) these data were complemented by a hydrological and meteorological measurement network that was installed during the years 2012 to 2015. Five automatic weather stations including pluviometers were installed in the catchment. The outlet of the catchment was equipped with a water level and turbidity probe. Precipitation and calculated potential evapotranspiration (ETp) are given as hourly time series for each of the five climate stations located in the studied catchment.

Furthermore, an extensive soil survey was conducted to analyze physical and chemical soil properties and to retrieve the soil and hydrological parameters required by the model.

Observed climate data for the period 1990–2015 were used to assess the influence of LULC change on hydrology and soil erosion. To cover the full period we used data with a daily resolution taken by the national meteorological service (Direction Général de la Météorologie du Burkina, DGM) (Fig. 1c).

2.2.2.2. Modeled climate data. Historical (1990–2005) and scenario-based (2006–2032) precipitation and temperature data were retrieved from the regional climate model (RCM) CCLM4–8 (Climate Limited-area Modelling Community, Germany) driven by the global climate model (GCM) ESM-LR (Max-Planck-Institute for Meteorology, Germany). The Representative Concentration Pathways RCP 4.5 and RCP 8.5 (Moss et al., 2010) were used as future scenarios. The RCM-GCM simulation was run in the framework of the Coordinated Regional climate Downscaling Experiment (CORDEX-Africa, www.cordex.org). Due to the run time of SHETRAN the closest node and one climate model was used only. The performance of other climate models and a discussion of the differences between nodes is given by Op de Hipt et al. (2018).

Historical precipitation and temperature data from CCLM-ESM model were compared with their observed counterparts for the period 1971–2000 to control if the modeled variables are in agreement with the observed. The modeled temperature shows a negative deviation compared to the observed temperature (Fig. 2a). As temperature is used to calculate potential evapotranspiration (Oudin et al., 2005) and has therefore strong effects on catchment hydrology, it was bias corrected using the delta change approach described in Haddeland et al. (2012) (Fig. 2b).

The comparison of modeled and observed precipitation indicates an obvious bias. Modeled precipitation is often higher than measured and a shift between the observed and the simulated timing of the rainy season can be observed (Fig. 2c). Therefore, a bias correction method was used to correct the historical and future rainfall data derived from CCLM-ESM. The non-parametric quantile mapping approach introduced by Gudmundsson et al. (2012) was applied. The observed data were used to establish a transfer function which was applied to the historical and the future rainfall data. The differences between mean monthly precipitation from all climate models and the observed precipitation are considerably reduced after bias correction (Fig. 2d).

The comparison of bias corrected precipitation and potential evapotranspiration between the periods 1990–2005 and 2006–2032 shows an increase of precipitation by 5.4% to 7.8% and an increase of ETp by 4.7% to 6%.

Because bias correction is done on monthly scale and because climate models simulate climate and not weather, it cannot be expected

Table 1
Initial LULC classes as given by Landmann et al. (2007) and Forkuor (2014) and reclassified classes used in this study.

Initial LULC classes	Proportional area [%] per year							Reclassified LULC classes
	1990	2000	2007	2013	2019	2025	2030	
Regularly flooded, woody, closed to open	1.03	29.2	–	–	–	–	–	Tree and shrub savannah
Broadleaved forest, closed, evergreen (≥65%)	1.77	–	–	–	–	–	–	Tree and shrub savannah
Woodland, closed (40–65%)	5.22	–	–	–	–	–	–	Tree and shrub savannah
Woodland closed/forest closed	59.3	–	8.80	–	–	–	–	Tree and shrub savannah
Reg. flooded, high confidence	1.16	–	–	–	–	–	–	Tree and shrub savannah
Burned area	4.03	2.64	–	–	–	–	–	Cropland
Bare soil scattered vegetation	1.00	–	–	–	–	–	–	Urban area
Regularly flooded wetland	0.84	–	–	–	–	–	–	Tree and shrub savannah
Herbaceous crops	8.28	–	–	–	–	–	–	Cropland
Herbaceous vegetation, closed (≥65%)	17.28	–	–	–	–	–	–	Tree and shrub savannah
Forest	–	3.45	15.5	–	–	–	–	Tree and shrub savannah
Grassland	–	35.1	46.7	–	–	–	–	Tree and shrub savannah
Cropland	–	16.1	20.4	36.3	42.3	48.3	54.5	Cropland
Wetland	–	13.2	1.52	–				Tree and shrub savannah
Urban area	–	0.16	6.54	5.19	7.19	9.19	11.1	Urban area
Water	–	–	0.42	0.39	0.39	0.39	0.39	Water
Natural/-semi-natural vegetation	–	–	–	58.1	50.0	42.0	33.9	Tree and shrub savannah

Table 2
Applied datasets and required inputs for SHETRAN.

Data set	Spatiotemporal resolution/scale	Source	Derived parameters
Topography	90 m	SRTM (Jarvis et al., 2008)	
Soil	1:25000	Soil survey	Soil hydrological parameters (α, n[a], K_{sat}[b], θ_{sat}[c], θ_{res}[d]) texture etc.
Land use maps	5 to 250 m	Forkuor (2014), Landmann et al. (2007)	Land use type distribution
Land use characteristic		Literature	LAI[e], Strickler coefficient, ETa/ETp ratio[f]
Meteorological data	Hourly, Daily	Instrumentation WASCAL, DGM[g], CORDEX[h]	Rainfall, temperature, humidity, solar radiation, wind speed
Discharge	Hourly	Instrumentation WASCAL	Discharge
Erosion	Hourly, Event	Instrumentation WASCAL	Suspended sediment load, soil erosion rate

[a] α and n are van Genuchten empirical parameters.
[b] K_{sat} refers to the saturated hydraulic conductivity.
[c] θ_{sat} to the saturated water content.
[d] θ_{res} to the residual water content.
[e] LAI to the leaf area index.
[f] ETp/ETa ratio to the ratio of potential evapotranspiration to actual evapotranspiration.
[g] Direction Général de la Météorologie du Burkina.
[h] Coordinated Regional climate Downscaling Experiment project.

that water and sediment fluxes using observed and modeled climate are identical although the underlying climate variables precipitation and temperature are statistically identical. Therefore, analysis of future climate can only be compared to the modeled and not the observed past.

2.3. Modeling approach

2.3.1. Model description, parameterization, calibration and validation

SHETRAN was selected in this study due to two main reasons. First, SHETRAN is able to simulate erosion on hillslopes as well as in the river, which are both considered as important processes in the catchment. Second, it simulates processes based on continuous time series, which is necessary to use climate change scenarios and for land use comparisons over a given period. SHETRAN is a physically based spatially distributed hydrological soil erosion model. It is a derivative of SHE (Système Hydrologique Européen), which was jointly developed by the British Institute of Hydrology, the Danish Hydraulic Institute and the French consulting company SOGREAH (Abbott et al., 1986). SHETRAN has been refined and complemented by new components as e.g. the fully 3D simulation of subsurface water flow (Parkin, 1996) and sediment transport (Wicks, 1988; Wicks and Bathurst, 1996). Detailed information is available online (http://research.ncl.ac.uk/shetran/).

Details on model parameterization, calibration and validation are given in Section 3.2 and Op de Hipt et al. (2017). The parameterization of soil properties was done based on data obtained from field measurements and additional literature analysis (Tables 2, 3). Land use parameters were taken from literature (see Table 3). Although SHETRAN comprises numerous parameters that reflect the influence of the vegetation on hydrology we focused on two parameters: i) the ratio of actual evapotranspiration (ETa) to potential evapotranspiration (ETp) and ii) the Strickler coefficient (KSTR) that were reported to be sensitive regarding surface runoff (Bathurst et al., 2004; Birkinshaw et al., 2010a; Đukić and Radić, 2016; Zhang, 2015). Erosion was described using four parameters (overland flow and rain drop soil erodibility coefficients, channel bank erodibility coefficient, threshold depth of loose sediment) that were adjusted based on literature (Adams and Elliott, 2006; Birkinshaw et al., 2010a; de Figueiredo and Bathurst, 2007; Elliott et al., 2011; Lukey et al., 2000, 1995; Norouzi Banis et al., 2004; Wicks and Bathurst, 1996) and calibration (Table 3).

Spatially distributed data, including a digital elevation model (DEM), the soil and land use map were used in a raster format with a grid

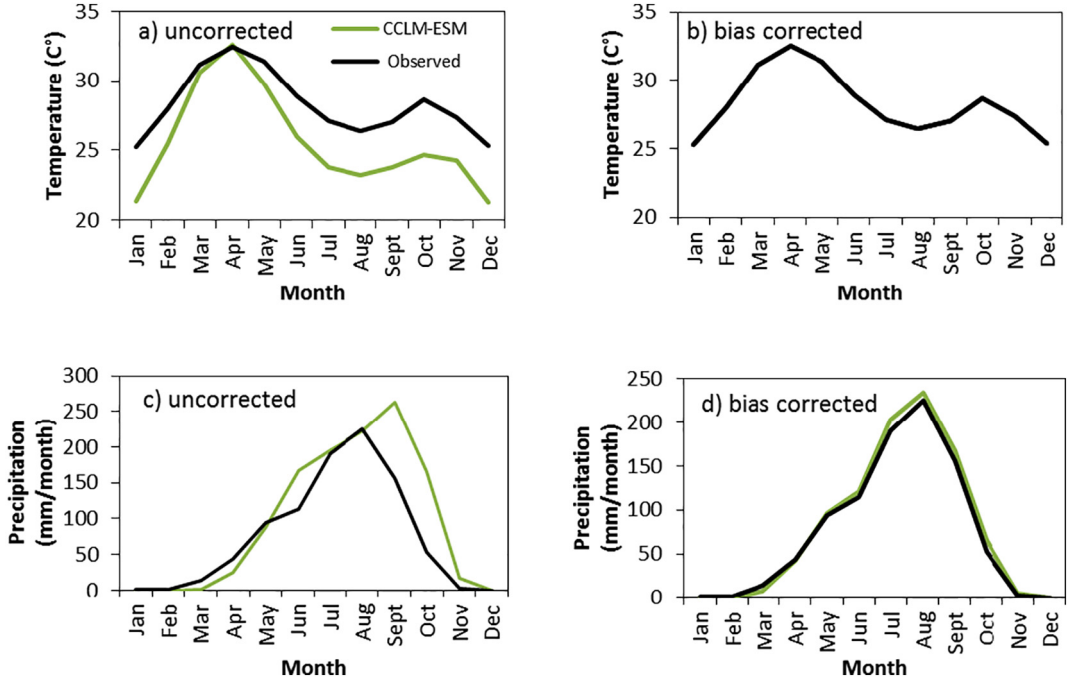

Fig. 2. Uncorrected and bias corrected temperature (a, b) and precipitation (c, d).

Table 3
Soil, land use and erosion parameters in SHETRAN ([1)]NV: natural vegetation (mainly savannah), [2)]CR: crop land, [3)]SM: settlement).

Parameter	Description	Unit	Parameter range	Source
Hydrology				
ETa/ETp at field capacity (varies with land use type)	Ratio of actual evapotranspiration to potential evapotranspiration at field capacity	–	CR[1)]: 0.5 NV[2)]: 0.6 SM[3)]: 0.1	Shuttleworth (1993)
KSTR (varies with land use type)	Strickler roughness coefficient	$m^{1/3}$ s^{-1}	CR: 1.4 NV: 0.6 SM: 6.0	Mohamoud (1992), Shen and Julien (1993)
Soil erosion				
k_f (soil invariant)	Overland flow soil erodibility	kg m^{-2} s^{-1}	7.5×10^{-11}	Calibration
k_r (varies with texture)	Raindrop soil erodibility coefficient	J^{-1}	0.19–7.9	Adams and Elliott (2006), Birkinshaw et al. (2010a), de Figueiredo and Bathurst (2007), Elliott et al. (2011), Lukey et al. (2000, 1995), Norouzi Banis et al. (2004), Wicks and Bathurst (1996)
BKB (soil invariant)	Channel bank erodibility coefficient	kg m^{-2} s^{-1}	1×10^{-6}–3×10^{-6}	Calibration
DLSMAX	Threshold depth of loose sediment	mm	1×10^{-6}–9.9×10^{-6}	Calibration

resolution of 200 × 200 m. An extensive soil survey was conducted to analyze physical and chemical soil properties and to retrieve the soil and hydrological parameters required by the model.

Although SHETRAN is physically based, land use and soil erosion related parameters needed to be calibrated to adjust for model approximations and the spatial or temporal resolution of the input data. In the present study six selected parameters (Table 3) were calibrated based on the Latin Hypercube Sampling (LHS) methodology (McKay et al., 1979). Briefly, using LHS the possible multi-dimensional parameter space is sampled n times (usually n > 100) in a stratified manner and the parameters are used in the simulation model to determine behavioral simulations (simulations which show an acceptable comparison with observed data). The hydrological component of SHETRAN was calibrated based on the observed hydrograph from 2014 to 2015. The soil erosion component was calibrated based on the observed suspended sediment load (SSL). The model performance was statistically evaluated by the coefficient of determination (R^2), the Nash-Sutcliff efficiency (NSE) (Nash and Sutcliffe, 1970) and the Kling-Gupta efficiency (KGE) (Gupta et al., 2009; Kling et al., 2012) because a single quality measure is not sufficient for model evaluation. The model was validated using data from the year 2015.

2.3.2. Model application and simulations

In this study, the model parameters and the boundary conditions remain unchanged for all simulations. Therefore, LULC and climate change is not reflected by changing parameters but the changing spatial patterns of the land cover classes and the changing climate data.

To evaluate the effects of changing land use and climate separately and their combined effects we applied over all 17 model simulations. As the periods 1984–1996 and 1984–1989 were used as the warm-up phase to reach hydrological equilibrium conditions, the period 1997–2032 (evaluation period) was used to evaluate the effect of LULC and climate change on average annual water components and on the average annual specific sediment yield. For the model warm-up climate data from 1984 to 1996 and the land use map LULC_1990 is applied. In order to compare simulations we used different evaluation periods as shown in Table 4.

Statistical differences between the selected model outputs (water yield, actual evapotranspiration, specific sediment yield) of each model run was investigated on a daily basis using the Kruskal-Wallis test. Pairwise comparisons were studied by applying the Bonfferoni correction to results of Mann-Whitney *U* tests.

The following points shortly describe each simulation. An overview of the different simulations is given in Table 4.

The model simulations of the past (simulations M1_1990–M5_90/13):

- The simulation M1_1990 is considered as the reference and applies the land use map LULC_1990 over the entire simulation period (1990–2005). Observed climate data are used to drive the simulation.
- Simulations M2_2000, M3_2007 and M4_2013 apply the observed land use maps from 2000, 2007 and 2013 to the period from 1997 to 2005. For each simulation the same observed climate data for the period from 1997 to 2005 are used. During each simulation the land cover did not change. Different simulation outputs are therefore the effect of different LULC data only. To be able to compare simulations M1_1990–M4_2013 with the simulations driven by past modeled climate data, we limited the evaluation period to 1997–2005.
- The simulation M5_90/13 applies the chronological land use development as it has occurred in the catchment. Therefore the LULC map from 1990 is applied to the period from 1990 to 1996, the map from 2000 applied to the period 1997–2003, the map from 2007 to the period 2004–2010 and finally the map from 2013 to the period 2011–2015. M5_90/13 uses the same observed climate data as simulations M1 to M4.

The model simulations of the future (simulations M6_2019–M17_90/13):

- Simulations M6_2019, M7_2025 and M8_2030 apply the modeled land use maps from 2019, 2025 and 2030 to the observed climate data from 1997 to 2005. In accordance with simulations M2 to M4, during each simulation LULC does not change and changes between each simulation are due to changing LULC, while each simulation applied the same observed climate data.
- The simulations M9_1990_RCP4.5 and M10_1990_RCP8.5 use modeled climate data (see Section 2.2.2) of the period 1990–2032 in combination with the land use map LULC_1990 assuming a constant LULC since 1990. Model runs M9 and M10 use modeled climate data and changes in fluxes are computed as differences between the modeled past (1990–2005) and the modeled future (2006–2032). These simulations enable the assessment of climate change as single factor. The periods 1990–2005 and 2006–2032 are compared regarding the effect of climate change on discharge and SSY.

Table 4
LULC simulations, model periods and applied land use maps.

Data	Simulation name	Simulation period						
		Warm-up period	Evaluation period					
		1990–1996	1997–2005			–	–	–
Observed climate and LULC maps	M1_1990	LULC_1990	LULC_1990			–	–	–
	M2_2000	LULC_1990	LULC_2000			–	–	–
	M3_2007	LULC_1990	LULC_2007			–	–	–
	M4_2013	LULC_1990	LULC_2013			–	–	–
		Warm-up period	Evaluation period					
		1990–1996	1997–2003	2004–2010	2011–2015			
	M5_90/13	LULC_1990	LULC_2000	LULC_2007	LULC_2013	–	–	–
Data	Simulation name	Warm-up period	Evaluation period					
		1990–1996	1997–2005					
Observed climate and modeled LULC maps	M6_2019	LULC_1990	LULC_2019			–	–	–
	M7_2025	LULC_1990	LULC_2025			–	–	–
	M8_2030	LULC_1990	LULC_2030			–	–	–
Data	Simulation name	Warm-up period	Evaluation period					
		1990–1996	1997–2005	2006–2010	2011–2016	2017–2022	2023–2027	2028–2032
Modeled climate and observed LULC map	M9_1990_RCP4.5	LULC_1990	LULC_1990					
	M10_1990_RCP8.5	LULC_1990	LULC_1990					
Modeled climate and modeled LULC maps	M11_90/30_RCP4.5	LULC_1990	LULC_2000	LULC_2007	LULC_2013	LULC_2019	LULC_2025	LULC_2030
	M12_90/30_RCP8.5	LULC_1990	LULC_2000	LULC_2007	LULC_2013	LULC_2019	LULC_2025	LULC_2030
Data	Simulation name	Warm-up period	Evaluation period					
		1984–1997	1998–2005					
Past modeled climate and observed LULC maps	M13_1990	LULC_1990	LULC_1990					
	M14_2000	LULC_1990	LULC_2000					
	M15_2007	LULC_1990	LULC_2007					
	M16_2013	LULC_1990	LULC_2013					
	Simulation name	Warm-up period	Evaluation period					
		1984–1989	1990–1997	1998–2005				
	M17_90/13	LULC_1990	LULC_1990	LULC_2000				

- A chronological and continuous application of all LULC maps (LULC_1990–LULC_2030) was only possible through the use of precipitation and temperature from a climate model (see Section 2.2.2). Modeled precipitation and temperature (1990–2032) in combination with LULC maps from 1990 to 2030 were used to drive the simulations M11_90/30_RCP4.5 and M12_90/30_RCP8.5. The periods 1990–2005 and 2006–2032 are compared regarding the effect of climate change on discharge and SSY.
- Simulations M13_1990–M17_90/13 are similar to simulations M1_1990–M5_90/13 except they use past modeled climate data from the period 1984–2005 and are necessary to evaluate the differences between the past modeled and observed climate data.

2.3.2.1. Timestep sensitvity. The long term meteorological data operated by the national meteorological service (see Fig. 1c) was only available on daily basis. This is critical since results of dynamic models such as

SHETRAN respond sensitively to the chosen simulation time step (Bruneau et al., 1995; Hessel, 2005; Yira, 2016; Zhang, 2015) and consequently the consideration of time and spatial scales is fundamental in hydrological modeling (Blöschl and Sivapalan, 1995). Yira (2016) reports a decreasing modeled discharge with increasing time step. This can be explained by the information loss during aggregation of rainfall data from sub-daily to daily resolution: It reduces the maximum intensities and therefore leads to an underestimation of overland flow due to infiltration excess as this depends on rainfall intensity and soil infiltration rate. Consequently, simulated discharge and hence sediment yield may be underestimated by the model. However, some SHETRAN studies also use a daily timestep (de Figueiredo and Bathurst, 2007; Mourato et al., 2015). Fig. 3 shows that the exceedance probability does not change substantially between two simulations with different timesteps. Although an increase in timestep reduces surface runoff and sediment yield, this limitation cannot be avoided for the long-term simulations as no hourly data are available. Because all scenarios are influenced by the same effect, conclusions drawn from the analysis are not biased by the temporal resolution of the model runs.

3. Results and discussion

3.1. Land use and land cover change

The LULC maps and changes of the period 1990–2030 are shown in Fig. 4. The observed LULC maps show an increase of mainly cropland and settlement area at the expense of savanna areas, which have decreased by almost 30% between 1990 (86.69%) and 2013 (58.12%) whereas cropland has increased by almost 24% in the same period. An urbanization trend is reflected by an increase in settlement areas by 4.1% between 1990 and 2013. The area covered by surface water increases between 2000 and 2007 as the Moutouri reservoir was built in 2002. The future LULC change (from 2019 to 2030) mainly follows the trend of the past. An increase of cropland (42.2%) and settlement areas (10.19%) between 1990 and 2030 is opposed to a decrease in savanna by 52.7%.

Some inconsistencies are observed regarding the spatial distribution of settlements derived from the past LULC maps. Between 1990 and 2000 settlement areas in the LULC map are reduced due to the unlikely conversion of settlements to savanna, water and cropland. Further unlike LULC changes are noticed between the maps from 2000 and 2007 where the settlement area is 25 fold increased over 7 years. The inconsistencies are of relatively low importance as the maximum proportion of cells characterized by an improbable change is <7%. The LULC mapping of savanna areas is impeded due to the seasonality and the scattered LULC pattern (Cord et al., 2010; Forkuor, 2014). Therefore, the observed inconsistencies can be explained by a misclassification related to the difficulties of the LULC mapping of areas characterized by a distinct seasonality (Wagner et al., 2013). Another reason may be the resampling of the maps needed to attain the same grid resolution which discriminates the scattered land use classes (Yira et al., 2016).

The large visual and numerical differences between LULC_2007 and the other maps rectified the exclusion of LULC_2007 for the derivation of the future LULC maps. Two important issues have to be discusses in this context: First, the future LULC development only depends on the change that occurred between 2000 and 2013. Second, the future LULC may be afflicted with large uncertainties because important variables as population growth and agronomical developments are not available to improve the predictions. However, based on observations from the field and personal communication with local farmers, factors as the distance to the farm house and the accessibility play an important role for cultivation.

An expansion of cropland at the expense of natural vegetation mainly due to increasing demand for agricultural areas as a result of the population growth and national migration is also reported by others (CILSS, 2016; Gray, 1999; Mahé et al., 2005; Ouedraogo et al., 2010; Paré et al., 2008; Stephenne and Lambin, 2001; Thiombiano and Kampmann, 2010). The present study assesses the increase of cropland by 0.95% per year while savanna is reduced by 1.14% per year for the observed period (1990–2013). Paré et al. (2008) studied the influence of population growth on land use change and reports conversion rates of 3.75% per year in the Sissili and Ziro provinces, which are located in approximately 100 km distance to the study area. Although the exact number differs the major driver controlling LULC change in the study area is population growth and urbanization trends, which is also reported on the national level (CILLS, 2016). Future LULC maps suggest an increase of cropland of 42.2% till 2030. This corresponds to the scenarios used by Hiepe (2008) who reports increases between 56%–119%. The deforestation in the catchment is directly related to the growing demand in firewood used among others for the production of local beer and remote areas are increasingly affected as the number of unprotected trees close to the main settlements diminishes. The logging of shea trees (*Vitellaria paradoxa*) used to produce shea butter for export may pose a problem in the future as it is an important financial income for small scale farmers. Another important cash crop is cotton whose production has increased by 350% since 1990 (FAOSTAT, 2017).

3.2. Performance of SHETRAN

The performance of SHETRAN regarding the hydrological and erosion modeling is discussed in Op de Hipt et al. (2017) and therefore only briefly summarized here. Based on the various performance measures (sum of R^2, KGE and NSE), several parameter sets gave satisfactory to good quality measures according to the equifinality concept introduced by Beven and Freer (2001). The given performance measures for discharge are in the range of 0.7 and 0.79 for calibration and between 0.66 and 0.76 for validation which is comparable to other studies that used SHETRAN (e.g. Birkinshaw et al., 2014; Đukić and Radić, 2016, 2014; Mourato et al., 2015; Naseela et al., 2015; Tripkovic, 2014; Zhang, 2015). Among these studies R^2 and NSE values above 0.5 are frequently reported. Larger differences between simulated and observed discharge occur during low flow conditions where the observed discharge is frequently underestimated by the model. This is not surprising since low flow was not in the focus and consequently parameters controlling low flow such as K_{sat} in sub-surface soils were not considered during the calibration. Overestimated peaks during the rainy season

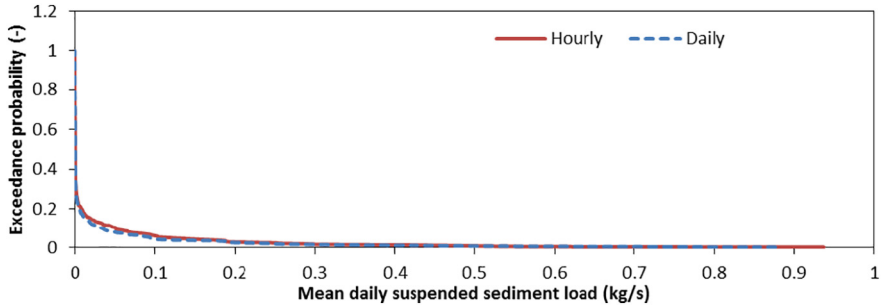

Fig. 3. Exceedance probability of hourly and daily suspended sediment load.

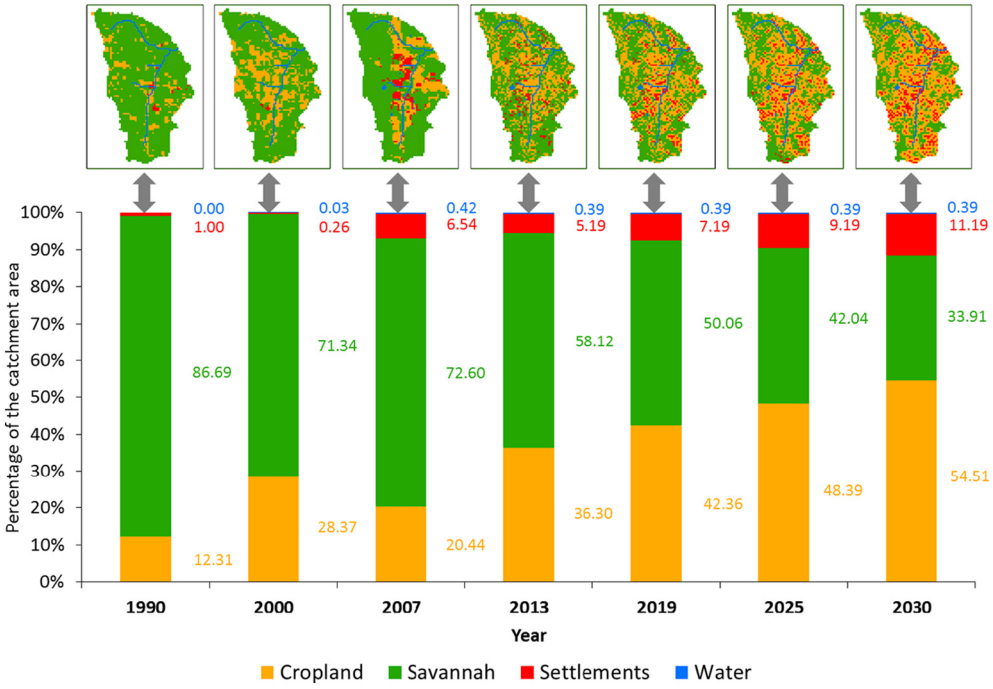

Fig. 4. Observed (1990–2013) and modeled (2019–2030) LULC maps and the corresponding relative proportion of each land use.

can be attributed to the spatial assignment of climate stations, which was done using Thiessen polygons. This method may not be appropriate to account for localized precipitation events. Nevertheless, alternative interpolations methods like inverse distance weighting and Kriging may also be inadequate to reflect local storms as they smooth rainfall intensities over larger spatial extends.

In terms of erosion rates the NSE is 0.4 and 0.2 and the R^2 is 0.47 and 0.37 for calibration and validation of SSL respectively. These results are in the range of other studies (de Figueiredo and Bathurst, 2007; Elliott et al., 2011; Zhang, 2015) and comparable with other erosion models (de Vente et al., 2013; Jetten et al., 1999). Given the various sources of measurement uncertainty a NSE of larger than 0.7 can't be expected (de Vente et al., 2013).

3.3. Land use and climate change effects

3.3.1. Hydrology

Fig. 5a, Tables 5, and 6 show the influence of land use on simulated mean annual water yield over the considered period (1997–2030). The simulations that were driven by the past observed climate and

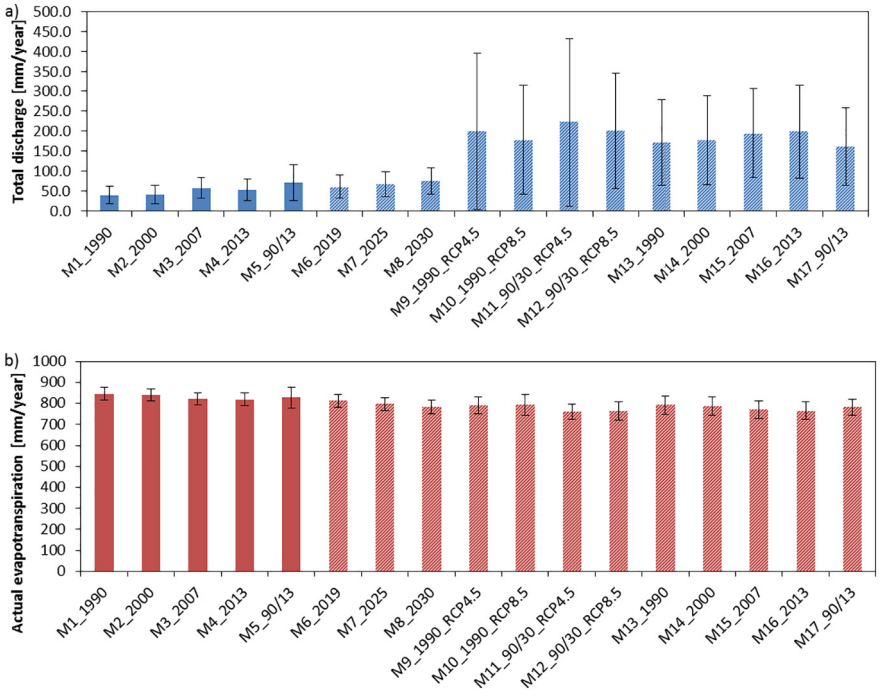

Fig. 5. a) Mean annual total water yield for M1_1990–M12_90/30_RCP8.5 and b) mean annual actual evapotranspiration for simulations M1_1990–M12_90/30_RCP8.5. Error bars indicate the standard deviation calculated based on annual sums. Dashed bars indicate the use of modeled LULC and/or climate. See Table 4 and the text for explanation of the different scenarios.

LULC maps (M1_1990–M5_90/13) indicate an increased water yield by 3.6% (M2_2000) to 46.4% (M3_2007) (evaluation period: 1997–2005). The water yield of the continuous simulation M5_90/13 is 20.3% higher compared to M1_1990 (evaluation period 1997–2015). It shows that LULC change over almost 20 years has affected the water balance of the studied catchment significantly.

Simulations driven by future modeled LULC maps and observed climate data (M6_2019–M8_2030) show highest increases in discharge between 52.4%–91.6% compared to M1_1990 (evaluation period: 1997–2005). Consequently, the predicted LULC change will lead to an increased discharge assuming a similar climate development as observed between 1990 and 2005.

Simulations M9_1990_RCP4.5 and M10_1990_RCP8.5 are driven by modeled climate data and the map LULC_1990 only, assuming no change of LULC since 1990. The comparison between simulated discharge of the period 1990–2005 and of the period 2006–2032 shows an increase of discharge between 24.5% (M10_1990_RCP8.5) and 46.7% (M9_1990_RCP4.5). The increased water yield is attributed to climate change only.

Simulations M11_90/30_RCP4.5 and M12_90/30_RCP8.5 are driven by a combined LULC and climate change. The comparisons of the periods 1990–2005 to the years 2006–2032 show high increases (50.5% (M12)–73.4% (M11)) of discharge. Consequently, the combined development of climate and LULC may intensify the future change of hydrological conditions in the catchment.

Simulations M13–M17 use past observed LULC maps and past modeled climate data. Accordingly, these simulations are needed to assess the influence of past modeled climate data and LULC change on water and sediment yield. M14_2000–M16_2013 show increases between 3.4% (M14) and 16.6% (M16) compared to M13_1990 (evaluation period: 1997–2005). The continuous simulation M17_90/13 show an increase of 1.5% compared to M13_1990 (evaluation period: 1990–2005).

The comparison between the groups M9/M10 (climate change only, +24.5%–+46.7%), M11/M12 (LULC and climate change, +50.5–+73.4%) and M13-M17 (LULC change only, +1.5%–+16.6%) shows that LULC change only leads to increases in water yield. When comparing LULC change and climate change alone it is clear that climate change has a larger impact but LULC amplifies climate change impacts strongly. However, future LULC (2019–2030) will have a stronger impact as currently observed. Furthermore, the comparison between M13–M17 and M1–M5 shows that the simulation driven by observed climate data (M1–M5) are characterized by higher percental increases than those simulations that are driven by modeled climate data from the past although precipitation is higher for M13–M17. The differences in relative change between the group M1–M5 and M13–M17 is related to differences in the absolute discharge which is about three times higher for M13–M17. Therefore, M13–M17 show a smaller relative change compared to M1–M5.

Statistically significant ($p < 0.0007$) differences exist between almost all pairs. Exceptions are M1_1990/M5_2013, M3_2007/M4_2013, and M11_90/30_RCP4.5/M12_90/30_RCP8.5.

The effect of LULC and climate change on ETa is shown in Fig. 5b. The simulations driven by observed data (M1_1990–M5_90/13) indicate that ETa decreases between 0.7% and 3.2%. Simulations that used modeled LULC maps and observed climate data (M6_2019–M8_2030) show decreasing ETa (4%–7.3%) compared to M1_1990 (evaluation period: 1997–2005). The simulations that use climatic predictions assuming constant LULC since 1990 (M9, M10) show an increasing ETa by between 3.1% (M9) and 3.3% (M10). A decreasing trend is predicted by the combined consideration of LULC and climate change as shown by simulations M11 (−1.58%) and M12 (−0.96%). Simulations M14_2000–M17_90/13 show the same trend as simulations M2–M5 with decreasing rates of ETa between 0.3% and 3.4%. The comparison between the pairs M9/M10 and M11/M12 suggests that LULC change may dominate the impact on ETa because the increasing trend as suggested by climate change only is reversed by the combined consideration of LULC and climate change. Significant ($p < 0.0007$) differences compared to the reference the simulation M1_1990 exist for the majority of considered pairs.

The presented figures for simulations M1_1990–M5_90/13 are similar to the results of Yira et al. (2016) who studied the influence of a changing LULC on the hydrology in the same area based on similar data using WASiM (Water Balance Simulation Model). He observed an increase in discharge of 20% between M1_1990 and M5_90/13. The general trend of increasing discharge and decreasing ETa is reported by others and LULC change was frequently responsible for this development (Bossa et al., 2014; Cornelissen et al., 2013; Mahé et al., 2005; Roudier et al., 2014; Yira et al., 2016). Bossa et al. (2014) studied the impact of climate and LULC change on hydrology in the Ouémé catchment in Benin. They assess the effect of different LULC scenarios on water yield to be between +3% and +8%. For the combined consideration of climate and LULC change they report a decreasing water yield over the period 2015–2019 according to the negative future precipitation signal. The influence of the future precipitation signal on water yield is also confirmed by Yira et al. (2017) and by the present study as CCLM-ESM shows a positive future signal for the considered period (2006–2032). However, conclusions drawn from simulations that use data from climate models have to be considered carefully as uncertainties of future precipitation predictions are large (Yira et al., 2017). Simulations M9 and M10 are afflicted with large inter-annual variabilities as indicated by the high standard deviation. These variabilities are a result from the precipitation as predicted by CCLM-ESM.

Regarding the consideration of LULC change only, the presented results are confirmed by experiments conducted on smaller scales. These experiments suggest that the increase of water yield due to land use change is attributed to a change of soil properties such as a decreasing K_{sat} leading to Hortonian surface runoff (Giertz et al., 2005; Yira, 2016). However, in SHETRAN K_{sat} varies with soil type and not with land use. Consequently, it remained unchanged over all simulations and cannot explain the differences between the simulations. Among the land use specific model parameters LAI, the vegetation cover fraction, the Strickler roughness coefficient (KSTR), and the ratio ETa/ETp were adjusted to the corresponding land use types to reflect their differences regarding the hydrological effects. In SHETRAN the roughness coefficient and the ratio ETa/ETp have distinct effects on discharge as shown by Op de Hipt et al. (2017) and Đukić and Radić (2016). Decreased surface roughness as observed on agricultural fields (Engman, 1986) results in higher surface runoff velocities and therefore especially influences the runoff peaks. However, interactions between surface

Table 5
Average annual water balance and specific suspended sediment yield of simulation driven by observed climate. The evaluation period from 1997 to 2005 is marked by *, the evaluation period from 1997 to 2015 is marked by **.

Simulation	M1_1990	M2_2000	M3_2007	M4_2013	M5_90/13	M6_2019	M7_2025	M8_2030
Mean annual rainfall [mm]	877*/903**	877*/903**	877*/903**	877*/903**	903**	877*/903**	877*/903**	877*/903**
Mean annual ETp [mm]	1826*/1809**	1826*/1809**	1826*/1809**	1826*/1809**	1809**	1826*/1809**	1826*/1809**	1826*/1809**
Mean annual ETa [mm]	846*/844**	840*/839**	821*/820**	818*/820**	827**	812*/822**	797*/802**	784*786**
Mean annual water yield [mm]	39.4*/59.4**	40.8*/61.7**	57.7*/81.2**	52.7*	71.4**	60*/86.7**	67.1*/95.5**	75.5*/105**
Mean annual specific suspended sediment yield [t/ha]	0.021*/0.0317**	0.021*/0.0312**	0.032*/0.0449**	0.031*/0.0445**	0.0395**	0.038*/0.0531**	0.043*/0.0599**	0.051*/0.0684**

Table 6
Average annual water balance and specific suspended sediment yield. Annual means of the modeled past (1990–2005)[a] and the modeled scenarios (2006–2032)[b] are indicated for simulations M9–M12. The evaluation period from 1998 to 2005 for M13–M17 is marked by *, the evaluation period from 1998 to 2015 is marked by **.

Simulation	M9_1990_RCP4.5	M10_1990_RCP8.5	M11_90/30_RCP4.5	M12_90/30_RCP8.5	M13_1990	M14_2000	M15_2007	M16_2013	M17_90/2005
Mean annual rainfall [mm]	951[a]–1026[b]	951[a]–1002[b]	951[a]–1026[b]	951[a]–1002[b]	997*/951**	997*/951**	997*/951**	997*/951**	951**
Mean annual ETp [mm]	1578[a]–1653[b]	1578[a]–1674[b]	1578[a]–1653[b]	1578[a]–1674[b]	1616*/1578**	1616*/1578**	1616*/1578**	1616*/1578**	1578**
Mean annual ETa [mm]	775[a]–799[b]	775[a]–801[b]	768[a]–756[b]	768[a]–761[b]	798*/784**	794*/780**	776*/763**	771*/758**	781**
Mean annual water yield [mm]	154[a]–226[b]	154[a]–192[b]	152[a]–264[b]	152[a]–229[b]	170.6*/157.9**	176.5*/164.7**	194.3*/182.3**	198.9*/187.5**	160.4**
Mean annual specific suspended sediment yield [t/ha]	0.084[a]–0.13[b]	0.084[a]–0.11[b]	0.082[a]–0.15[b]	0.082[a]–0.13[b]	0.097*/0.09**	0.099*/0.102**	0.112*/0.11**	0.120*/0.087**	0.087**

roughness, infiltration and evapotranspiration also lead to a change of water yield. The ratio ETa/ETp, which depends on the vegetation type and varies with soil water tension, has strong effects on the water balance components. A higher actual evapotranspiration on natural land use types is frequently reported (e.g. Compaoré, 2006). Other vegetation properties such as LAI or vegetation cover also influence the discharge. Decreasing LAI and vegetation cover leads to more throughfall, which may increase surface runoff.

3.3.2. Soil erosion

Fig. 6, Tables 5 and 6 show the effect of LULC and climate change on the mean annual specific suspended sediment yield (SSY). Simulations driven by observed data (M1_1990–M5_90/13) show a change of SSY between −3.3% (M2_2000) and +52.6% (M3_2007) for the evaluation period 1997–2005. The relative contribution of each land use type to the catchment erosion varies between M1_1990 and M5_90/13 (evaluation period: 1997–2015): The relative contribution of cropland increases by 11% whereas the contribution of savanna decreases by 9% as a result of the changing proportion of each land use type. The channel contribution varies between 42% (M4_2013) and 51% (M1_1990) suggesting that if the contribution of hillslope erosion increases the channel contribution decreases. Among the sediment sources water also contributes to the sediment yield of the catchment. The model structure only allows a limited number of soil types and an additional soil type reflecting the conditions of areas covered by water could not be implemented. The continuous simulation M5_90/13 exhibits an increase of 24.7% compared to the reference simulation M1_1990 suggesting that LULC change has already a pronounced impact on soil erosion (evaluation period: 1997–2015).

Simulations driven by future modeled LULC maps and observed climate data (M6_2019–M8_2030) show highest increases in SSY between 78.5% (M6_2019) and 138.4% (M8_2030) compared to M1_1990 (evaluation period: 1997–2005). Consequently, the predicted LULC change will lead to an increased SSY assuming a similar climate development as observed between 1990 and 2005. The proportion of the different sources remains roughly similar between M6–M8 except for savanna whose contribution decreases by 6%.

The simulation M9_1990_RCP4.5 and M10_1990_RCP8.5 reflect a changing climate assuming stable LULC since 1990. The periods 1990–2005 and 2006–2032 are used for the comparison. The simulations show that the predicted change in precipitation (+5.4% to +7.8%), ETa (+3.1% to +3.3%) and accordingly water yield (+24.5% to +46.7%) strongly influence SSY. Both, water yield and SSY are strongly correlated as surface runoff is the principal driver of sediment transport. Overall SSY is predicted to increase by 31.1% (M10_1990_RCP8.5) and 54.7% (M9_1990_RCP4.5). Table 5 shows that these increases are especially attributed to the scenario-based predictions (2005–2030). Furthermore, the source distribution indicates that these increases are especially caused by a substantial increase of channel contribution compared to the other simulations.

The continuous simulations M11_90/30_RCP4.5 and M12_90/30_RCP8.5 reflect the combined impact of LULC and climate change on SSY. Overall SSY is predicted to increase by 67.7% (M12_90/30_RCP8.5) to 90.1% (M11_90/30_RCP4.5) compared to the period 1990–2005.

Simulations M14_2000–M16_2013 show increases by between 2.1% and 23.3% compared to simulation M13_1990 (evaluation period: 1997–2005). These changes are lower compared to the results of simulations M1-M5 although absolute precipitation is higher for M13–M17. This is attributed to the absolute amount of SSY which almost 3 times higher for simulation M13–M15.Simulation M17_90/13 are driven by past modeled climate data and observed LULC maps of 1990 and 2000. The relative change between M13 and M17 is almost 0%.

The comparison between the groups M9/M10 (climate change only, +31.1–+54.7%), M11/M12 (climate and LULC change, +67.7%–+90.1%) and M13 - M17 (LULC change only, 0%–+23.3%) suggest that

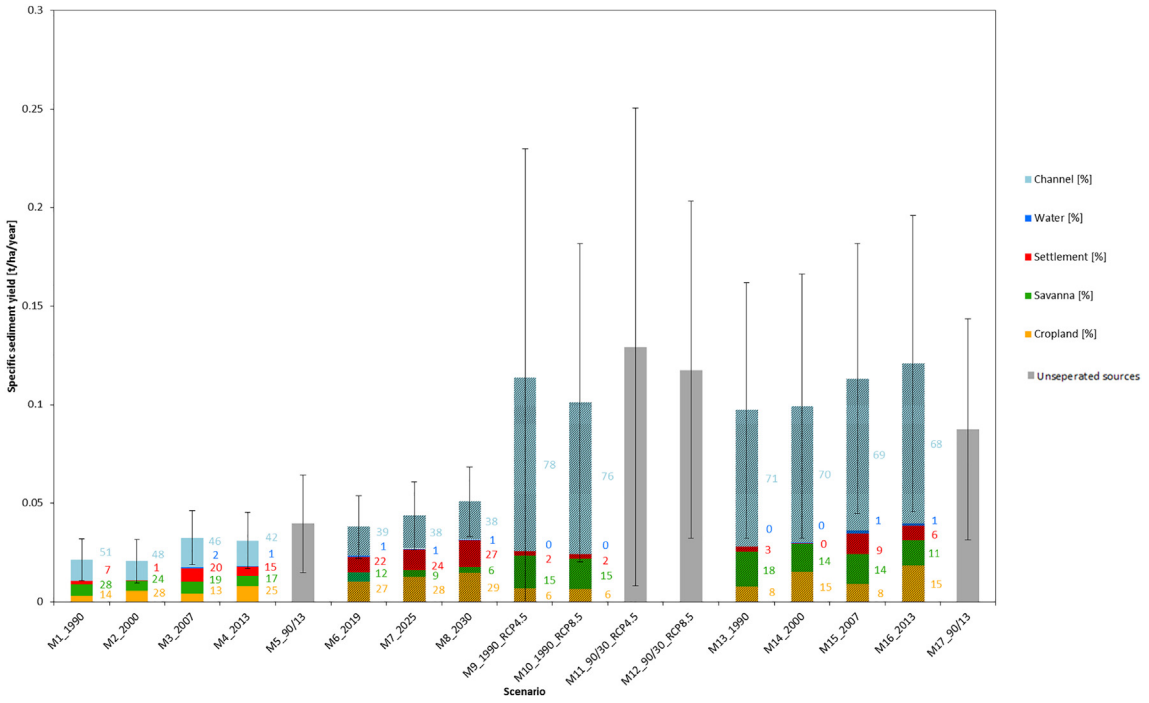

Fig. 6. Mean annual specific suspended sediment yield for the simulations M1_1990–M12_90/30_RCP8.5. The contribution of each source is given in % for all simulations except for the continuous simulations (M5, M11, M12, M17). Error bars indicate the standard deviation calculated based on annual sums. Dashed bars indicate the use of modeled LULC maps and/or modeled climate data.

LULC change may have a large impact on SSY. Simulations driven by climate change only (M9/M10) show higher increases than those simulations that were driven by LULC change (M13–M17). However, climate change impacts are significantly amplified by LULC change as shown by simulations M11/M12. All of the discussed simulations are statistically different except the pairs M3/M4 and M11/M12. However, uncertainties of LULC and climate predictions have to be discussed. Simulations M9 to M12 are characterized by high inter-annual variabilities. This is mostly related to large uncertainties of predicted precipitation. The impact of climate change on the rainfall pattern and temperature in West Africa is difficult to assess and differences between climate models regarding amplitude and direction exists (Kasei et al., 2010; Niang et al., 2014). This uncertainty is among others attributed to the difficulties of simulating convective rainfalls and the rainfalls generated by the West African Monsoon (WAM) which is attributed to the incomplete knowledge of the WAM, lack of observations and the natural climate variability in the region (Cook, 2008; Druyan et al., 2010; Field and Barros, 2014; Klein et al., 2015; Niang et al., 2014).

From Fig. 6 and the described results it can be concluded that LULC and climate change are important drivers that control the catchment sediment yield and the corresponding erosion sources. Increased erosion rates following a conversion from natural vegetation to cropland are frequently confirmed by measurements and simulations in the region (e.g. Bossa et al., 2014; Giertz et al., 2005; Hiepe, 2008). Giertz et al. (2005) compared the influence of different crops and natural vegetation on soil erosion and concluded that increased surface runoff on cropland resulted in increased soil loss on agricultural fields compared to the savanna environment. The increased surface runoff can be explained by the reduction of macroporosity as result of decreased biological activity following the disturbance of the soil by agricultural activities. Furthermore, farming leads to a decreased soil quality parameters (Braimoh and Vlek, 2004) as e.g. a loss of soil organic matter which destabilizes soil aggregates and facilitates surface crusting resulting in a decreased infiltration rate (Descroix et al., 2009; Valentin et al., 2004). However, this process chain is not simulated by SHETRAN. Bossa et al. (2014) investigated the effect of LULC and climate change on sediment yield in the Ouémé catchment in Benin. Their modeling approach included the SWAT model, climate data from REMO and five LULC maps from 2003 to 2029. The combined application of LULC and climate change suggests an increase of SSY by 6% to 41% (Bossa et al., 2014). Differences between their results and ours can be explained by the different climate model (CCLM-ESM vs. REMO) and by the different modeling approach (SHETRAN vs. SWAT).

The simulated specific sediment yields are quite low for all simulations (<0.13 t/ha). In this context it is important to notice, that we consider the suspended fraction only. Furthermore, the term soil erosion is differentiated from sediment yield. Soil erosion refers to soil detachment and not necessarily soil loss from a specific area. Sediment yield refers to the amount of eroded soil that is transported to a certain point in the catchment. However, the simulated suspended sediment yields are comparable with specific suspended sediment yields measured in 2014 (0.04–0.13 t/ha/year) especially if the large simulated inter-annual variability is considered. The problem of low simulated SSY is already discussed in Op de Hipt et al. (2017) and may also be attributed to the parameterization of the erosion component and the insufficient representation of space and time in the model approach. However, the adjustment of the erosion parameters in a way that they reflect the natural conditions is quite challenging due to limited knowledge of the parameter ranges and of the erosion processes and source distribution especially in West Africa. Schmengler (Schmengler, 2010; Schmengler and Vlek, 2015) studied soil erosion in the same catchment by comparing sedimentation rates in 3 headwater sub-catchments (7.9–23.6 km^2). Two of her studied headwater catchments show lower SSY (0.3 t/ha/year–0.8 t/ha/year). They are representative of the typical flat terrain (2°–3°). The third headwater catchment is located in the western part and is characterized by steeper slope gradients (up to 20°) which leads to substantially higher SSY (4.4 t/ha/year). The mean slope of our study catchment is 1.8 and therefore comparable to the two catchments showing a low annual SSY. The differences compared to our results can be explained by the different fractions considered and the topographical position. Schmengler (2010) investigated reservoirs located in the headwater areas. Consequently, her measured

SSY is only valid for these topographical positions and possible sedimentation downslope is not considered.

The contribution of channels to the mean annual SSY seems to be quite high (51–76%) for all simulations. However, recent results from fingerprinting analyses which were conducted in 2013 and 2014 support the modeling result for the past. The contribution of subsurface sources ranges 44% and 47% (Michael Rode, personal communication, 14th July 2017).

4. Conclusion

The present study investigated the LULC and climate change in the Dano catchment and its effects on catchment hydrology and soil erosion using the process based SHETRAN model, which was driven by past (observed) and future (modeled) LULC maps and modeled and observed climate data. The main results of this study are:

1. The most important land use change in the catchment is the conversion from savanna to cropland. The study of the observed LULC maps (1990–2013) shows an annual conversion rate of savanna of 1.14% since 1990. The future LULC maps (2019–2030) predict an increase of cropland by 42.2% compared to 1990.
2. The analysis of the isolated impact of the LULC change on catchment hydrology clearly suggests an increase of mean annual water yield (3.6%–91.6%) and a decrease of mean annual ETa (0.7–7.3%) while the proportion of cropland increases. The comparison between simulations suggests that the impact of future climate (24.5–46.7%) may be amplified by the inclusion of LULC change (50.5–73.4%). However, uncertainties of climate model outputs have to be considered. The combined effect of LULC and climate change leads to a decrease in ETa (0.96%–1.58%).
3. The investigation of the isolated effect of LULC changes on specific suspended sediment yield (SSY) over the period 1990–2030 mostly shows an increasing trend (−3.6–138.4%) which is supported by measurements and modeling studies. The increase of SSY is mostly attributed to the enlarging cropland, which also forms an important and growing contribution source to total catchment erosion. The comparison of the isolated impact of climate change and the combined effect of climate and LULC change suggest that the inclusion of LULC change may amplified the climate change impacts. The combined impact of LULC and climate change results in high changes of SSY (+67.7%–+90.1%).

The obtained modeling results highlight the negative effects of the conversion of natural vegetation to cropland or settlements on catchment hydrology and soil loss independent whether observed or modeled past climate data were used. The conversion results in less infiltration, higher surface runoff and soil loss as well as lower groundwater recharge. However, the present findings are based on results of hydrological and soil erosion modeling driven by LULC and climate data which are subject to uncertainties. The observed LULC maps were produced based on different satellite products and needed to be reclassified. The afflicted uncertainties are propagated as these maps are the basis for the development of future LULC scenarios. The precipitation as modeled by climate models is frequently considered as uncertain as shown by comparison studies. Furthermore, the modeling approach is based on the changing spatial proportion of the different land use types only and does not consider the complex processes and feedback loops between land use changes, soil properties, hydrology, and soil erosion. Consequently, the results must be carefully interpreted even if the model was validated in terms of discharge and suspended sediment load. A focus should be put to relative and not the absolute comparisons between the simulations. This relative comparison signals a clear effect of LULC and climate change on hydrology and soil erosion.

In addition to the related uncertainties possible implications need to be discussed. The predicted changes of the hydrological cycle and the altered sediment budget may have implications for different fields as for example agricultural productivity or water availability. However, a discussion based on measured data is beyond the scope and possibilities of the present work. Therefore, the following discussion of possible implications includes results from previous studies.

A clear link has been identified between soil erosion, soil fertility, agricultural production and food security (Niang et al., 2014; Pimentel, 2006). García-Fayos and Bochet (2009) studied the impact of climate change on the interaction between soil erosion and different soil and vegetation properties in semiarid Mediterranean shrublands in eastern Spain. Their analyses suggest that the negative impact of climate change and increased soil erosion on vegetation properties (species richness and plant cover) negatively affects soil erodibility, nutrient content and water holding capacity which may lead to a decline of soil and agricultural productivity. The negative impact of climate change on soil erosion and agricultural yields was proven by Zhang et al. (2004) for experimental sites in Oklahoma, USA. They used modeled climate data and the WEPP model to simulate the effect of climate change on soil erosion and wheat yield. A similar study was conducted by Li et al. (2011) for the Loess Plateau in China. Their results suggest that plant yields may increase despite increased erosion rates due to the fertilization effects of CO_2. Paeth et al. (2008) studied the impact of climate change on soil degradation and agricultural production in Benin using REMO data and predict a decline in crop yield of up to 23% due to soil erosion. A similar range of projected decreasing yields are reported by Butt et al. (2005) for Mali. Our results show that it is not possible to identify a clear positive or negative trend regarding the future erosion rates. Therefore, it is also difficult to consult decision makers regarding adaption strategies for an appropriate agricultural management. Based on the studies presented above we can conclude that a climate or LULC induced increase of erosion rates may have negative effects on soil fertility, agricultural production and ultimately food security. Thus, governmental support of soil and water conservation measures such as stone lines, intercropping or the traditional Zaï system (Roose et al., 1999) would be necessary to increase the environmental resilience of this region. In view of the low SSY on hillslopes and the large contribution of channel erosion as simulated by SHETRAN (Fig. 6) it may be questionable if the increased erosion rates will significantly affect agricultural production. Our modeling results and findings from a recent fingerprinting campaign suggest that a substantial part (about 50%) of the sediment loss in the catchment results from bank erosion and river incision. However, the above mentioned conservation techniques may also decrease surface runoff and hence discharge in the channels which in turn may lead to decreased bank erosion and river incision. This would also decrease the off-site effects on reservoirs located downstream as reservoir siltation is recognized as a serious problem (Schmengler, 2010).

However, it is debatable if results from modeling studies conducted on a rather large scale and coarse temporal and spatial resolution can be used to derive specific advices for decision makers on the local scale because these results are rather valid on the catchment scale and do not perfectly reflect the local diversity regarding the catchment properties but also the different processes. As such SHETRAN considers already important processes but some observations from the field are not well reflected. This considers for example the role of inland valleys which are rather sediment sinks for material eroded on upstream as observations from the field suggest. Furthermore, these observations suggest that soil properties and erosion processes differ on very small scales and the coarse spatial resolution we had to use may limit the transfer from model results to locally implementable advices for decision makers. Therefore, the current modeling study underlines future research demands for climate model projections with smaller uncertainties. As specific advices for decision makers should be based on several independent research studies we also emphasize the need for further research regarding feedback loops between climate change, LULC change, soil erosion and.

Acknowledgements

The authors are grateful for the financial support provided by the German Federal Ministry of Education and Research (BMBF) (Grant No. 01LG1202E) under the auspices of the West African Science Service Centre for Climate Change and Adapted Land Use (WASCAL) project. Furthermore, we thank Stephen Birkinshaw (School of Engineering, Newcastle University) for his kind support regarding the set-up of SHETRAN. We acknowledge the soil sampling and mapping done by Ozias Hounkpatin (Soil Science of Institute of Crop Science and Resource Conservation, University Bonn). We also thank the CORDEX project and partner institutions for making climate data available and D. Wisser for providing a R-code for bias correction.

References

Abbott, M.B., Bathurst, J.C., Cunge, J.A., O'Connell, P.E., Rasmussen, J., 1986. An introduction to the European Hydrological System — Systeme Hydrologique Europeen, "SHE", 1: history and philosophy of a physically-based, distributed modelling system. J. Hydrol. 87, 45–59. https://doi.org/10.1016/0022-1694(86)90114-9.

Adams, R., Elliott, S., 2006. Physically based modelling of sediment generation and transport under a large rainfall simulator. Hydrol. Process. 20, 2253–2270. https://doi.org/10.1002/hyp.6050.

Bathurst, J.C., Ewen, J., Parkin, G., O'Connell, P.E., Cooper, J.D., 2004. Validation of catchment models for predicting land-use and climate change impacts. 3. Blind validation for internal and outlet responses. J. Hydrol. 287, 74–94. https://doi.org/10.1016/j.jhydrol.2003.09.021.

Bathurst, J.C., Moretti, G., El-Hames, A., Moaven-Hashemi, A., Burton, A., 2005. Scenario modelling of basin-scale, shallow landslide sediment yield, Valsassina, Italian Southern Alps. Nat. Hazards Earth Syst. Sci. 5, 189–202. https://doi.org/10.5194/nhess-5-189-2005.

Bathurst, J.C., Birkinshaw, S.J., Cisneros, F., Fallas, J., Iroumé, A., Iturraspe, R., Novillo, M.G., Urciuolo, A., Alvarado, A., Coello, C., Huber, A., Miranda, M., Ramirez, M., Sarandón, R., 2011. Forest impact on floods due to extreme rainfall and snowmelt in four Latin American environments 2: model analysis. J. Hydrol. 400, 292–304. https://doi.org/10.1016/j.jhydrol.2010.09.001.

Beven, K., Freer, J., 2001. Equifinality, data assimilation, and uncertainty estimation in mechanistic modelling of complex environmental systems using the GLUE methodology. J. Hydrol. 249, 11–29. https://doi.org/10.1016/S0022-1694(01)00421-8.

Birkinshaw, S.J., Bathurst, J.C., Iroumé, A., Palacios, H., 2010a. The effect of forest cover on peak flow and sediment discharge — an integrated field and modelling study in central–southern Chile. Hydrol. Process. 25, 1284–1297. https://doi.org/10.1002/hyp.7900.

Birkinshaw, S.J., James, P., Ewen, J., 2010b. Graphical user interface for rapid set-up of SHETRAN physically-based river catchment model. Environ. Model. Softw. 25, 609–610. https://doi.org/10.1016/j.envsoft.2009.11.011.

Birkinshaw, S.J., Bathurst, J.C., Robinson, M., 2014. 45 years of non-stationary hydrology over a forest plantation growth cycle, coalburn catchment, Northern England. J. Hydrol. 519 (Part A), 559–573. https://doi.org/10.1016/j.jhydrol.2014.07.050.

Blöschl, G., Sivapalan, M., 1995. Scale issues in hydrological modelling: a review. Hydrol. Process. 9, 251–290. https://doi.org/10.1002/hyp.3360090305.

Bossa, A., 2012. Multi-scale modeling of sediment and nutrient flow dynamics in the Ouémé catchment (Benin) - towards an assessment of global change effects on soil degradation and Water Quality. (Phd thesis). Rheinische Friedrich-Wilhelms-Universität Bonn, Bonn http://hss.ulb.uni-bonn.de/2012/2983/2983.htm.

Bossa, A., Diekkrüger, B., Agbossou, E., 2014. Scenario-based impacts of land use and climate change on land and water degradation from the meso to regional scale. Water 6, 3152–3181. https://doi.org/10.3390/w6103152.

Braimoh, A.K., Vlek, P.L.G., 2004. The impact of land-cover change on soil properties in northern Ghana. Land Degrad. Dev. 15, 65–74. https://doi.org/10.1002/ldr.590.

Bruneau, P., Gascuel-Odoux, C., Robin, P., Merot, P., Beven, K., 1995. Sensitivity to space and time resolution of a hydrological model using digital elevation data. Hydrol. Process. 9, 69–81. https://doi.org/10.1002/hyp.3360090107.

Butt, T.A., McCarl, B.A., Angerer, J., Dyke, P.T., Stuth, J.W., 2005. The economic and food security implications of climate change in Mali. Clim. Chang. 68, 355–378. https://doi.org/10.1007/s10584-005-6014-0.

Chan, J.C., Chan, K., Yeh, A.G., 2001. Detecting the nature of change in an urban environment: a comparison of machine learning algorithms. Photogramm. Eng. Remote. Sens. 67, 213–225.

CILSS (Comité Inter-états de Lutte contre la Sécheresse dans le Sahel), 2016. Landscapes of West Africa - A Window on a Changing World. U.S. Geological Survey EROS, Garretson, United States.

Codjoe, S.N.A., 2004. Population and Land Use, Cover Dynamics in the Volta River Basin of Ghana: 1960–2010. Cuvillier Verlag.

Compaoré, H., 2006. The Impact of Savannah Vegetation on the Spatial and Temporal Variation of the Actual Evapotranspiration in the Volta Basin, Navrongo, Upper East Ghana. Cuvillier.

Cook, K.H., 2008. Climate science: the mysteries of Sahel droughts. Nat. Geosci. 1, 647–648. https://doi.org/10.1038/ngeo320.

Cord, A., Conrad, C., Schmidt, M., Dech, S., 2010. Standardized FAO-LCCS land cover mapping in heterogeneous tree savannas of West Africa. J. Arid Environ. 74, 1083–1091. https://doi.org/10.1016/j.jaridenv.2010.03.012.

Cornelissen, T., Diekkrüger, B., Giertz, S., 2013. A comparison of hydrological models for assessing the impact of land use and climate change on discharge in a tropical catchment. J. Hydrol. 498, 221–236. https://doi.org/10.1016/j.jhydrol.2013.06.016.

Descroix, L., Mahé, G., Lebel, T., Favreau, G., Galle, S., Gautier, E., Olivry, J.C., Albergel, J., Amogu, O., Cappelaere, B., 2009. Spatio-temporal variability of hydrological regimes around the boundaries between Sahelian and Sudanian areas of West Africa: a synthesis. J. Hydrol. 375, 90–102. https://doi.org/10.1016/j.jhydrol.2008.12.012.

Diekkrüger, B., 2010. Hydrological processes and soil degradation in Benin. In: Speth, P., Christoph, M., Diekkrüger, B. (Eds.), Impacts of Global Change on the Hydrological Cycle in West and Northwest Africa. Springer, Berlin.

Druyan, L.M., Feng, J., Cook, K.H., Xue, Y., Fulakeza, M., Hagos, S.M., Konaré, A., Moufouma-Okia, W., Rowell, D.P., Vizy, E.K., Ibrah, S.S., 2010. The WAMME regional model intercomparison study. Clim. Dyn. 35, 175–192. https://doi.org/10.1007/s00382-009-0676-7.

Đukić, V., Radić, Z., 2014. GIS based estimation of sediment discharge and areas of soil erosion and deposition for the torrential Lukovska River catchment in Serbia. Water Resour. Manag. 28, 4567–4581. https://doi.org/10.1007/s11269-014-0751-7.

Đukić, V., Radić, Z., 2016. Sensitivity analysis of a physically based distributed model. Water Resour. Manag. 30, 1669–1684. https://doi.org/10.1007/s11269-016-1243-8.

Elliott, A.H., Oehler, F., Schmidt, J., Ekanayake, J.C., 2011. Sediment modelling with fine temporal and spatial resolution for a hilly catchment. Hydrol. Process. 26, 3645–3660. https://doi.org/10.1002/hyp.8445.

Engman, E.T., 1986. Roughness coefficients for routing surface runoff. J. Irrig. Drain. Eng. 112, 39–53. https://doi.org/10.1061/(ASCE)0733-9437(1986)112:1(39).

Ewen, J., Parkin, G., O'Connell, P.E., 2000. SHETRAN: distributed river basin flow and transport modeling system. J. Hydrol. Eng. 5, 250–258. https://doi.org/10.1061/(ASCE)1084-0699(2000)5:3(250).

FAOSTAT, 2017. Burkina Faso [WWW Document]. URL. http://www.fao.org/faostat/en/#country/233, Accessed date: 16 February 2017.

Field, C.B., Barros, V.R. (Eds.), 2014. Climate Change 2014: Impacts, Adaptation, and Vulnerability. Cambridge University Press, New York, NY.

de Figueiredo, E.E., Bathurst, J.C., 2007. Runoff and sediment yield predictions in a semi-arid region of Brazil using SHETRAN. Proceedings of the PUB Kick-off Meeting. Presented at the PUB Kick-off Meeting. IAHS, Brasilia, Brazil.

Forkuor, G., 2014. Agricultural Land Use Mapping in West Africa Using Multi-sensor Satellite Imagery. (Phd thesis). Julius-Maximilians-Universität, Würzburg, Germany https://opus.bibliothek.uni-wuerzburg.de/frontdoor/index/index/docId/10868.

García-Fayos, P., Bochet, E., 2009. Indication of antagonistic interaction between climate change and erosion on plant species richness and soil properties in semiarid Mediterranean ecosystems. Glob. Chang. Biol. 15, 306–318. https://doi.org/10.1111/j.1365-2486.2008.01738.x.

Giertz, S., Junge, B., Diekkrüger, B., 2005. Assessing the effects of land use change on soil physical properties and hydrological processes in the sub-humid tropical environment of West Africa. Phys. Chem. Earth A/B/C 30, 485–496. https://doi.org/10.1016/j.pce.2005.07.003.

Giertz, S., Hiepe, C., Steup, G., Sintondji, L., Diekkrüger, B., 2010. Hydrological processes and soil degradation in Benin. In: Speth, P., Christoph, M., Diekkrüger, B. (Eds.), Impacts of Global Change on the Hydrological Cycle in West and Northwest Africa. Springer, Berlin.

Gray, L.C., 1999. Is land being degraded? A multi-scale investigation of landscape change in southwestern Burkina Faso. Land Degrad. Dev. 10, 329–343. https://doi.org/10.1002/(SICI)1099-145X(199907/08)10:4<329::AID-LDR361>3.0.CO;2-I.

Gudmundsson, L., Bremnes, J.B., Haugen, J.E., Engen-Skaugen, T., 2012. Technical Note: downscaling RCM precipitation to the station scale using statistical transformations - a comparison of methods. Hydrol. Earth Syst. Sci. 16, 3383–3390. https://doi.org/10.5194/hess-16-3383-2012.

Gupta, H.V., Kling, H., Yilmaz, K.K., Martinez, G.F., 2009. Decomposition of the mean squared error and NSE performance criteria: implications for improving hydrological modelling. J. Hydrol. 377, 80–91. https://doi.org/10.1016/j.jhydrol.2009.08.003.

Haddeland, I., Heinke, J., Voß, F., Eisner, S., Chen, C., Hagemann, S., Ludwig, F., 2012. Effects of climate model radiation, humidity and wind estimates on hydrological simulations. Hydrol. Earth Syst. Sci. 16, 305–318. https://doi.org/10.5194/hess-16-305-2012.

Hessel, R., 2005. Effects of grid cell size and time step length on simulation results of the Limburg soil erosion model (LISEM). Hydrol. Process. 19, 3037–3049. https://doi.org/10.1002/hyp.5815.

Hiepe, C., 2008. Soil Degradation by Water Erosion in a Sub-humid West-African Catchment - A Modelling Approach Considering Land Use and Climate Change in Benin. (Phd thesis). Rheinische Friedrich-Wilhelms-Universität Bonn, Bonn http://hss.ulb.uni-bonn.de/2008/1628/1628.htm.

IUSS Working Group, 2006. World reference base for soil resources 2006. World Soil Resources Reports, 2nd ed. FAO, Rome, Italy.

Jarvis, A., Reuter, H.I., Nelson, A., Guevara, E., 2008. Hole-filled SRTM for the Globe Version 4. (Available from the CGIAR-CSI SRTM 90m Database (http://srtm.csi.cgiar.org)).

Jetten, V., de Roo, A., Favis-Mortlock, D., 1999. Evaluation of field-scale and catchment-scale soil erosion models. Catena 37, 521–541. https://doi.org/10.1016/S0341-8162(99)00037-5.

Kasei, R., Diekkrüger, B., Leemhuis, C., 2010. Drought frequency in the Volta Basin of West Africa. Sustain. Sci. 5, 89–97. https://doi.org/10.1007/s11625-009-0101-5.

Klein, C., Heinzeller, D., Bliefernicht, J., Kunstmann, H., 2015. Variability of West African monsoon patterns generated by a WRF multi-physics ensemble. Clim. Dyn. 45, 2733–2755. https://doi.org/10.1007/s00382-015-2505-5.

Kling, H., Fuchs, M., Paulin, M., 2012. Runoff conditions in the upper Danube basin under an ensemble of climate change scenarios. J. Hydrol. 424–425, 264–277. https://doi.org/10.1016/j.jhydrol.2012.01.011.

Landmann, T., Herty, C., Dech, S., Schmidt, M., Dech, S., Schmidt, M., Vlek, P., 2007. Land cover change analysis within the GLOWA Volta basin in West Africa using 30-meter Landsat data snapshots. 2007 IEEE International Geoscience and Remote Sensing Symposium. Presented at the International Geoscience and Remote Sensing Symposium, Barcelona, pp. 5298–5301 https://doi.org/10.1109/IGARSS.2007.4424058.

Li, Z., Liu, W.-Z., Zhang, X.-C., Zheng, F.-L., 2011. Assessing the site-specific impacts of climate change on hydrology, soil erosion and crop yields in the Loess Plateau of China. Clim. Chang. 105, 223–242. https://doi.org/10.1007/s10584-010-9875-9.

Lukey, B.T., Sheffield, J., Bathurst, J.C., Lavabre, J., Mathys, N., Martin, C., 1995. Simulating the effect of vegetation cover on the sediment yield of mediterranean catchments using SHETRAN. Phys. Chem. Earth 20, 427–432. https://doi.org/10.1016/0079-1946(95)00056-9.

Lukey, B., Sheffield, J., Bathurst, J., Hiley, R., Mathys, N., 2000. Test of the SHETRAN technology for modelling the impact of reforestation on badlands runoff and sediment yield at Draix, France. J. Hydrol. 235, 44–62. https://doi.org/10.1016/S0022-1694(00)00260-2.

Mahé, G., Paturel, J.-E., Servat, E., Conway, D., Dezetter, A., 2005. The impact of land use change on soil water holding capacity and river flow modelling in the Nakambe River, Burkina-Faso. J. Hydrol. 300, 33–43. https://doi.org/10.1016/j.jhydrol.2004.04.028.

McKay, M.D., Beckman, R.J., Conover, W.J., 1979. A comparison of three methods for selecting values of input variables in the analysis of output from a computer code. Technometrics 21, 239–245. https://doi.org/10.2307/1268522.

Merritt, W.S., Letcher, R.A., Jakeman, A.J., 2003. A review of erosion and sediment transport models. Environ. Model. Softw. 18, 761–799. https://doi.org/10.1016/S1364-8152(03)00078-1.

Mohamoud, Y.M., 1992. Evaluating Manning's roughness coefficients for tilled soils. J. Hydrol. 135, 143–156. https://doi.org/10.1016/0022-1694(92)90086-B.

Moss, R.H., Edmonds, J.A., Hibbard, K.A., Manning, M.R., Rose, S.K., van Vuuren, D.P., Carter, T.R., Emori, S., Kainuma, M., Kram, T., Meehl, G.A., Mitchell, J.F.B., Nakicenovic, N., Riahi, K., Smith, S.J., Stouffer, R.J., Thomson, A.M., Weyant, J.P., Wilbanks, T.J., 2010. The next generation of scenarios for climate change research and assessment. Nature 463, 747–756. https://doi.org/10.1038/nature08823.

Mourato, S., Moreira, M., Corte-Real, J., 2015. Water resources impact assessment under climate change scenarios in Mediterranean watersheds. Water Resour. Manag. 29, 2377–2391. https://doi.org/10.1007/s11269-015-0947-5.

Naseela, E.K., Dodamani, B.M., Chandran, C., 2015. Estimation of runoff using NRCS-CN method and SHETRAN model. Int. Adv. Res. J. Sci. Eng. Technol. 2, 23–28. https://doi.org/10.17148/IARJSET.2015.2807.

Nash, J.E., Sutcliffe, J.V., 1970. River flow forecasting through conceptual models part I — a discussion of principles. J. Hydrol. 10, 282–290. https://doi.org/10.1016/0022-1694(70)90255-6.

Niang, I., Ruppel, O.C., Abdrabo, M.A., Essel, A., Lennard, C., Padgham, J., Urquhart, P., 2014. Africa. In: Barros, V.R., Field, C.B., Dokken, D.J., Mastrandrea, M.D., Mach, K.J., Bilir, T.E., Chatterjee, M., Ebi, K.L., Estrada, Y.O., Genova, R.C., Girma, B., Kissel, E.S., Levy, A.N., MacCracken, S., Mastrandrea, P.R., White, L.L. (Eds.), Climate Change 2014: Impacts, Adaptation, and Vulnerability. Part B: Regional Aspects. Cambridge University Press, Cambridge, United Kingdom and New York, NY, USA, pp. 1199–1265.

Norouzi Banis, Y., Bathurst, J.C., Walling, D.E., 2004. Use of caesium-137 data to evaluate SHETRAN simulated long-term erosion patterns in arable lands. Hydrol. Process. 18, 1795–1809. https://doi.org/10.1002/hyp.1447.

Op de Hipt, F., Diekkrüger, B., Steup, G., Yira, Y., Hoffmann, T., Rode, M., 2017. Applying SHETRAN in a tropical West African catchment (Dano, Burkina Faso)—calibration, validation, uncertainty assessment. Water 9, 101. https://doi.org/10.3390/w9020101.

Op de Hipt, F., Diekkrüger, B., Steup, G., Yira, Y., Hoffmann, T., Rode, M., 2018. Modeling the impact of climate change on water resources and soil erosion in a tropical catchment in Burkina Faso, West Africa. Catena 163, 63–77. https://doi.org/10.1016/j.catena.2017.11.023.

Oudin, L., Hervieu, F., Michel, C., Perrin, C., Andréassian, V., Anctil, F., Loumagne, C., 2005. Which potential evapotranspiration input for a lumped rainfall–runoff model? J. Hydrol. 303, 290–306. https://doi.org/10.1016/j.jhydrol.2004.08.026.

Ouedraogo, I., Tigabu, M., Savadogo, P., Compaoré, H., Odén, P.C., Ouadba, J.M., 2010. Land cover change and its relation with population dynamics in Burkina Faso, West Africa. Land Degrad. Dev. 21, 453–462. https://doi.org/10.1002/ldr.981.

Paeth, H., Capo-Chichi, A., Endlicher, W., 2008. Climate change and food security in tropical West Africa – a dynamic-statistical modelling approach. Erdkunde 62, 101–115. https://doi.org/10.3112/erdkunde.2008.02.01.

Pandey, A., Himanshu, S.K., Mishra, S.K., Singh, V.P., 2016. Physically based soil erosion and sediment yield models revisited. Catena 147, 595–620. https://doi.org/10.1016/j.catena.2016.08.002.

Paré, S., Söderberg, U., Sandewall, M., Ouadba, J.M., 2008. Land use analysis from spatial and field data capture in southern Burkina Faso, West Africa. Agric. Ecosyst. Environ. 127, 277–285. https://doi.org/10.1016/j.agee.2008.04.009.

Parkin, G., 1996. A Three-dimensional Variably-saturated Subsurface Modelling System for River Basins. (Phd thesis). Newcastle University, Newcastle upon Tyne, United Kingdom, Newcastle upon Tyne https://theses.ncl.ac.uk/dspace/handle/10443/3161.

Pimentel, D., 2006. Soil erosion: a food and environmental threat. Environ. Dev. Sustain. 8, 119–137. https://doi.org/10.1007/s10668-005-1262-8.

Roose, E., Kabore, V., Guenat, C., 1999. Zai practice: a West African traditional rehabilitation system for semiarid degraded lands, a case study in Burkina Faso. Arid Soil Res. Rehabil. 13, 343–355. https://doi.org/10.1080/089030699263230.

Roudier, P., Ducharne, A., Feyen, L., 2014. Climate change impacts on runoff in West Africa: a review. Hydrol. Earth Syst. Sci. 18, 2789–2801. https://doi.org/10.5194/hess-18-2789-2014.

Schmengler, A.C., 2010. Modeling Soil Erosion and Reservoir Sedimentation at Hillslope and Catchment Scale in Semi-arid Burkina Faso. (Phd thesis). Rheinische Friedrich-Wilhelms-Universität Bonn, Bonn http://hss.ulb.uni-bonn.de/2011/2483/2483.htm.

Schmengler, A.C., Vlek, P.L., 2015. Assessment of accumulation rates in small reservoirs by core analysis, ^{137}Cs measurements and bathymetric mapping in Burkina Faso. Earth Surf. Process. Landf. 40, 1951–1963. https://doi.org/10.1002/esp.3772.

Shen, H.W., Julien, P.Y., 1993. Erosion and sediment transport. In: Maidment, D.R. (Ed.), Handbook of Hydrology. McGraw-Hill, New York.

Shuttleworth, W.J., 1993. Evaporation. In: Maidment, D.R. (Ed.), Handbook of Hydrology. McGraw-Hill, New York.

Stephenne, N., Lambin, E.F., 2001. A dynamic simulation model of land-use changes in Sudano-sahelian countries of Africa (SALU). Agric. Ecosyst. Environ. 85, 145–161. https://doi.org/10.1016/S0167-8809(01)00181-5.

The World Bank, 2017. Burkina Faso | Data [WWW Document]. Burkina Faso URL. http://data.worldbank.org/country/burkina-faso, Accessed date: 16 February 2017.

Thiombiano, A., Kampmann, D., 2010. Biodiversity Atlas of West Africa, Volume II: Burkina Faso (No. II) (Ouagadougou & Frankfurt/Main).

Tripkovic, V., 2014. Quantifying and Upscaling Surface and Subsurface Runoff and Nutrient Flows Under Climate Variability. (Phd thesis). Newcastle University, Newcastle upon Tyne https://theses.ncl.ac.uk/dspace/handle/10443/2380.

UNEP (United Nations Environmental Programme), 2012. Global Environment Outlook 4 (No. 4). UNEP, Valletta, Malta.

Valentin, C., Rajot, J.-L., Mitja, D., 2004. Responses of soil crusting, runoff and erosion to fallowing in the sub-humid and semi-arid regions of West Africa. Agric. Ecosyst. Environ. 104, 287–302. https://doi.org/10.1016/j.agee.2004.01.035.

de Vente, J., Poesen, J., Verstraeten, G., Govers, G., Vanmaercke, M., Van Rompaey, A., Arabkhedri, M., Boix-Fayos, C., 2013. Predicting soil erosion and sediment yield at regional scales: where do we stand? Earth Sci. Rev. 127, 16–29. https://doi.org/10.1016/j.earscirev.2013.08.014.

Wagner, P.D., Kumar, S., Schneider, K., 2013. An assessment of land use change impacts on the water resources of the Mula and Mutha Rivers catchment upstream of Pune, India. Hydrol. Earth Syst. Sci. 17, 2233–2246.

Wicks, J.M., 1988. Physically-based Mathematical Modelling of Catchment Sediment Yield. (Phd thesis). Newcastle University, Newcastle upon Tyne https://theses.ncl.ac.uk/dspace/handle/10443/152.

Wicks, J.M., Bathurst, J.C., 1996. SHESED: a physically based, distributed erosion and sediment yield component for the SHE hydrological modelling system. J. Hydrol. 175, 213–238. https://doi.org/10.1016/S0022-1694(96)80012-6.

Wilson, C.O., Weng, Q., 2011. Simulating the impacts of future land use and climate changes on surface water quality in the Des Plaines River watershed, Chicago Metropolitan Statistical Area, Illinois. Sci. Total Environ. 409, 4387–4405. https://doi.org/10.1016/j.scitotenv.2011.07.001.

Yira, Y., 2016. Modelling Climate and Land Use Change Impacts on Water Resources in the Dano Catchment (Burkina Faso, West Africa). (Phd thesis). Rheinische Friedrich-Wilhelms-Universität Bonn, Bonn http://hss.ulb.uni-bonn.de/2017/4583/4583.htm.

Yira, Y., Diekkrüger, B., Steup, G., Bossa, A.Y., 2016. Modeling land use change impacts on water resources in a tropical West African catchment (Dano, Burkina Faso). J. Hydrol. 537, 187–199. https://doi.org/10.1016/j.jhydrol.2016.03.052.

Yira, Y., Diekkrüger, B., Steup, G., Bossa, A.Y., 2017. Impact of climate change on hydrological conditions in a tropical West African catchment using an ensemble of climate simulations. Hydrol. Earth Syst. Sci. 21, 2143–2161. https://doi.org/10.5194/hess-21-2143-2017.

Zhang, R., 2015. Integrated modelling for Evaluation of Climate Change Impacts on Agricultural Dominated Basin. (Phd thesis). University Evora, Evora https://dspace.uevora.pt/rdpc/handle/10174/13270.

Zhang, X.-C., Nearing, M.A., Garbrecht, J.D., Steiner, J.L., 2004. Downscaling monthly forecasts to simulate impacts of climate change on soil erosion and wheat production. Soil Sci. Soc. Am. J. 68, 1376. https://doi.org/10.2136/sssaj2004.1376.